Appropriate Evaluation of Primary Frequency Response and Its Applications

Chengwen Zhang, Hongyu Li, Zhihao Jiang, Weikang Wang, Chujie Zeng, Chang Chen, He Yin, Yilu Liu
Department of Electrical Engineering and Computer Science
University of Tennessee, Knoxville
Knoxville, TN, USA
czhang70@vols.utk.edu

Mark Baldwin
Dominion Energy
Glen Allen, VA, USA
mark.w.baldwin@dominionenergy.com

***Abstract*—Primary frequency response is a quintessential component that stabilizes power systems amid active power disturbances. However, the strength of primary frequency response, as calculated with disturbance events, shows a low consistency from event to event. Thus, its effectiveness as a system strength measure is questionable. This work shows that consistency and improved accuracy can be achieved on a statistical basis via event filtering. Event MW estimation and primary frequency response trending analyses are the applications presented in this paper. Synchronized field measurements in the Eastern Interconnection, powered by FNET/GridEye, are used for validation of the analyses and applications.**

***Index Terms*—Primary frequency response, synchronized measurement, FNET/GridEye, MW estimation, trending analysis.**

I. Introduction

Power systems rely on various frequency responses to stabilize the system when disturbances threaten the balance of generation and demand. Typically, these responses are categorized as inertial response, primary frequency control, secondary frequency control, and tertiary control [1]. The inertial response is instant by its nature due to the electromagnetic link between the rotors and stators. Primary, secondary, and tertiary controls are enabled by dedicated control schemes to arrest the frequency decline, recover the frequency level, and correct the area control error. Among the three control schemes, primary frequency control is at the forefront during the frequency dynamics as it confines the magnitude of frequency deviation, prevents load shedding, and maintains stability.

As power systems around the world are embracing a low-emission future, renewable energy resources interfaced by inverters are taking an increasingly important role in the generation fleets. For example, in the Eastern Interconnection, the generation from wind and solar reached 9% of the total generation from all fuel types. The ratios are higher in WECC, ERCOT, and power interconnections in Europe [2-4]. While the fast control capabilities of the inverters have the potential to be leveraged as frequency dynamic improvement measures, most of the resources interfaced with the grids today are not fully committed to frequency regulation due to concerns over lost opportunity cost, equipment aging cost, and stability issues [5]. This brings uncertainties to the safety margin of the power systems amid frequency dynamics. Hence, continuous assessment and monitoring of primary frequency response are critical for both system operators and planners.

On the one hand, appropriate assessment and monitoring provide critical information for the evaluation of trends of the primary frequency response. Together with the data of the generation mix during the same period, this provides system operators and planners with knowledge about how different types of generation fleets impact the overall performance of primary frequency response in a power system. The correlation between the primary frequency response and the changing generation mix provides enhanced awareness about the state of the system today and helps prepare for the changes coming in the future.

On the other hand, the appropriate and up-to-date evaluation of primary frequency response is also important for disturbance MW estimation. For example, the FNET/GridEye, hosted at the University of Tennessee and the Oak Ridge National Laboratory, monitors disturbances and sends out alerts to industrial partners and regulatory authorities in real time as the events happen [6], [7]. The MW size of the event will be important information for the operators and authorities in the decision-making and post-event analysis. An accurate, up-to-date primary frequency response strength estimate is the critical parameter that dictates the accuracy of the MW size estimation.

However, the primary frequency response of a power system, as observed by disturbance events, tends to be significantly volatile. Researchers have found scattered patterns of the events on the MW-Δf plane [8], [9]. The low correlation between the MW size and the frequency deviation, which are the two quantities used for the estimation of the strength of primary frequency response, leads to lower confidence in the estimated β (strength of primary frequency response in MW/0.1Hz) and obscures the trends in β.

This work was supported by Dominion Energy. This work also made use of Engineering Research Center Shared Facilities supported by the Engineering Research Center Program of the National Science Foundation and Department of Energy under NSF Award Number EEC-1041877 and the CURENT Industry Partnership Program.

2023 IEEE PES GTD International Conference and Exposition (GTD) | 978-1-7281-7025-1/23/$31.00 ©2023 IEEE | DOI: 10.1109/GTD49768.2023.00049

Therefore, this paper first identifies important factors that may hinder the effective and consistent assessment of the β values. Then, the application of such knowledge in primary frequency trending analysis and MW size estimation are discussed. The analysis, as well as validation, takes advantage of the FNET/GridEye's historical field data collected by its synchronized measurement network. While the examples provided in this paper are from the Eastern Interconnection, the methods and conclusions can be general for other large-scale power interconnections as well.

The rest of the paper is organized as follows: section II introduces the FNET/GridEye system and data preprocessing procedures. Section III discusses factors that have a significant impact on the estimation of primary frequency response β. Section IV gives examples of how the acquired knowledge about these factors can be applied to β trending analysis and event MW estimation for improved accuracy and consistency. Section V concludes the paper.

II. FNET/GridEye and Data Preprocessing

A. Introduction to FNET/GridEye

FNET is a wide-area monitoring system deployed at distribution-level networks. Its sensors are single-phase PMUs designed for plug-in installation at 120 V or 220 V outlets in ordinary homes and offices. The synchronized phasor measurements are sent back to data centers at the University of Tennessee and the Oak Ridge National Laboratory through internet connections. There are currently about 200 sensors deployed in the United States and Canada and about 80 sensors in major power grids around the world. Fig. 1 shows the current deployment of FNET/GridEye synchronized sensors in North America.

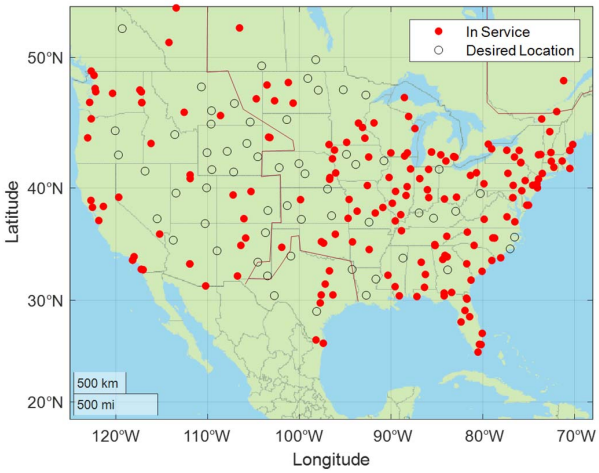

Figure 1. Deployment of FNET/GridEye sensors in North America

FNET/GridEye enabled a variety of applications, including real-time visualization, event triangulation, islanding alert, damping control, and large-scale power system model validation [10-20]. In this study, the raw, timestamped frequency measurement data from the sensors in the Eastern Interconnection are used for analysis and validation.

B. Data Preprocessing

Data preprocessing is a critical step before the measurement from the field can be used for analysis. First, the data should be properly treated for measurement noise and data loss as a result of communication uncertainties at the time of collection. Low-pass filters, interpolations, and curve fitting methods are commonly used by researchers to mitigate the impact of noise and data incompleteness [21], [22]. Then, in large-scale power interconnections, the inhomogeneity in frequency dynamics over vast geographical areas should be accounted for in the analysis. In this study, a sufficient quantity of FNET/GridEye sensors allows the use of the median filter to greatly reduce the impact of measurement error and to present near-inertia-center frequency dynamics. The median frequency filter accomplishes this by taking the median value of frequency measurements reported from all sensors at every sampling step as the representative frequency of the interconnection.

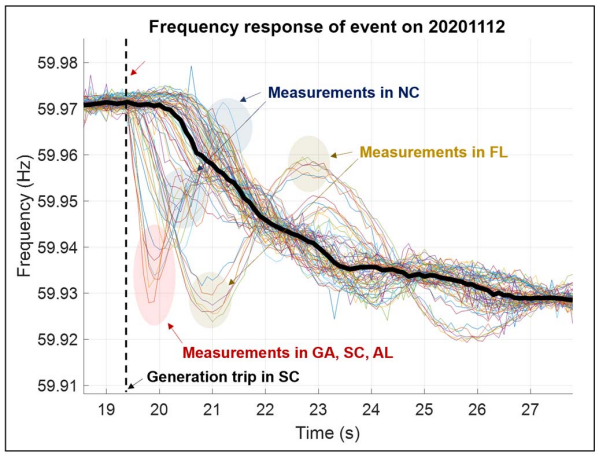

Figure 2 Regional frequency dynamics and median frequency

The disturbance event shown in Fig. 2 is an example of frequency inhomogeneity in large-scale power interconnections and how the median filter helps mitigate the impact of noise and oscillations. The regional frequency decline started instantly at the commencement of the disturbance, and then nearby regions followed. There was a significant amount of oscillation in states near the fault location. The noise and oscillations can significantly influence the observation of frequency dynamics on the interconnection level if only a limited number are available in confined areas. The coverage of FNET/GridEye sensors enables effective mitigation of these signal components, as shown by the black bold curve in Fig. 2. The median frequency curve will be used in the following text for analysis of the interconnection-level primary frequency response.

III. Analysis of Factors Impacting the Observed Primary Frequency Response

Unlike the inertial response, which is instant and mostly uniform to all events, the primary frequency response can be more complicated due to the existence of numerous governors that controls the generators' response to frequency deviations. Governors are often configured with frequency dead bands to

avoid unnecessary actions to frequently speed up or slow down generation in response to small perturbations [1].

Fig. 3 shows the two most common types of dead band configurations, the continuous output dead band, and the step output dead band.

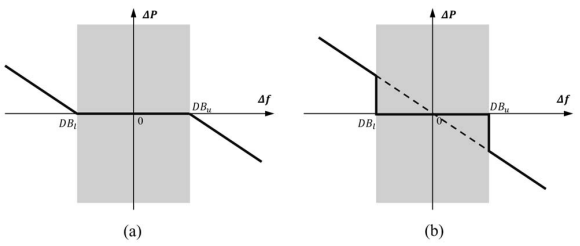

(a) Non-step output dead band (b) Step output dead band

Figure 3 Illustration of governor dead bands

In Eastern Interconnection, most of the generator units are configured with dead bands within the ± 36 mHz limits as recommended by the NERC standard [1]. While typically traditional coal plants are configured near 59.964 Hz, a large number of gas-fired units commissioned in recent years are configured with dead bands from 10 mHz to 17 mHz. Considering the distribution of governor dead bands in the interconnection, the primary frequency response to a disturbance event may vary widely depending on how the event interacts with these dead bands.

An intuitive expectation is the higher the pre-disturbance frequency is, the larger the frequency deviation becomes. This is because less primary frequency response from governors is engaged in the early stage of the frequency decline as it is within a large portion of governors' dead bands. This leads to a lower exhibition of the primary frequency response. In contrast, the lower the pre-disturbance frequency is, the smaller the frequency deviation will be since the governors are activated early on, leading to a stronger exhibition of primary frequency response.

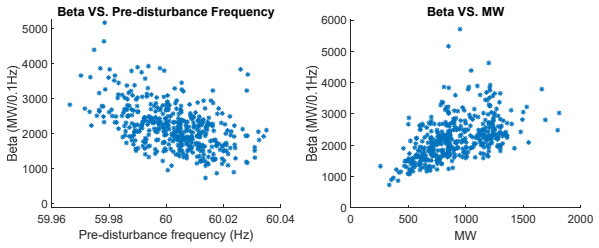

(a) β vs. f_{pre} (b) β vs. MW

Figure 4 Plot of β against pre-disturbance frequency and MW size

The two plots in Fig. 4 are scatter plots of β against pre-disturbance frequency and β against event MW size. It is clearly shown that there is a negative correlation between the β and pre-disturbance frequency, and a positive correlation between β and MW size. The correlation between β and f_{pre}, MW can be quantified with polynomial curve-fitting:

$$\hat{\beta} = p_0 \cdot MW^2 + p_1 \cdot MW \cdot f_{pre} + p_2 \cdot MW + p_3 \cdot f_{pre} + p_4 \quad (1)$$

where $p_0 = -166.1$, $p_1 = -130.2$, $p_2 = 450.5$, $p_3 = -432.7$, $p_4 = 2321$, and the pre-disturbance frequency and the MW size are normalized with their average values and standard deviations:

$$f_{pre} = \frac{f_{pre0} - \mu_{f_{pre0}}}{\sigma_{f_{pre0}}}, \qquad MW = \frac{MW_0 - \mu_{MW_0}}{\sigma_{MW_0}} \quad (2)$$

The normalization parameters are: $\mu_{f_{pre0}} = 60$, $\sigma_{f_{pre0}} = 0.01315$, $\mu_{MW_0} = 875$, $\sigma_{MW_0} = 260.1$. Equation (1) represents the curved surface that is fitted to the event data points, as shown in Fig. 5 (viewed from two angles).

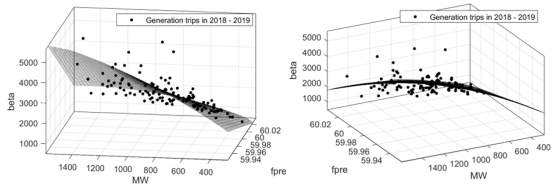

Figure 5 Fitting for β against f_{pre} and MW

The correlation coefficient of the fitting between β and f_{pre}, MW was as high as 0.831, which indicates that the pre-disturbance frequency and the event MW size are indeed two significant factors that impact the primary frequency response a disturbance event receives.

IV. Applications and Validations

The knowledge about the strong correlation between β and f_{pre}, MW has the potential for applications in various scenarios. In this paper, its application to beta trending analysis and online event MW estimation are discussed.

A. Improved Primary Frequency Response Trending Studies

The authors propose that the strength of primary frequency response, as observed through disturbance events, is contingent on the event's pre-disturbance frequency and MW size.

If so, these factors will have a significant impact on the effective and consistent evaluation of β. To demonstrate this, a year's worth of generation trip events are used as a group for calculation of the yearly β with least-square error estimates:

$$\hat{\beta} = (\boldsymbol{\Delta F^T \Delta F})^{-1} \cdot \boldsymbol{\Delta F^T} \cdot \boldsymbol{MW}$$
$$\boldsymbol{\Delta F} = [\Delta f_1, \Delta f_2, \dots, \Delta f_n]^T = [\Delta f_1, \Delta f_2, \dots, \Delta f_n]^T \quad (3)$$
$$\boldsymbol{MW} = [MW_1, MW_2, \dots, MW_n]^T$$

where $\boldsymbol{\Delta F}$ is the vector composed of frequency deviation magnitudes and $\boldsymbol{MW}$ the active power mismatch caused by the disturbances.

Fig. 6 (a) shows the $MW - \Delta f$ plot for the generation trip events in the year 2019. The blue dots represent individual generation trip events, and the red solid line is the yearly β obtained with the least-square fitting method in (3).

It is noted that the events are widely scattered on the $MW - \Delta f$ plane with a maximum individual β of 5164 MW/0.1Hz and a minimum individual β of 1097 MW/0.1Hz. Such a high degree of scatteredness undermines the credibility of the yearly β obtained. With the knowledge of how the event specifications

affect the exhibition of primary frequency response, event filters can be applied to select specific events for a more consistent comparison of β values across the years. For example, Fig. 6 (b) is the $MW - \Delta f$ plot of the 2019 events after being filtered with $59.995\ Hz < f_{pre} < 60.005\ Hz$ and $MW > 850$.

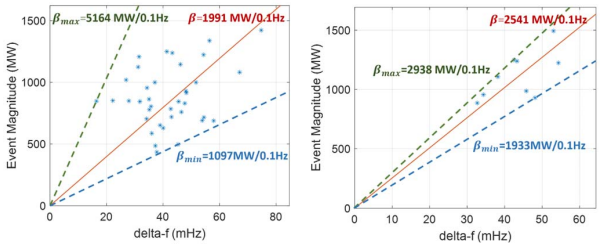

(a) before event filter (b) after event filter

Figure 6 $MW - \Delta f$ plot of generation trip events in year 2019

It is noted that the remaining events are concentrated around the least-square fitting curve. The correlation coefficient between MW and Δf improved to 0.822 (very strong correlation) from 0.467 (moderate-weak correlation). Table I includes critical statistics of the primary frequency response β before and after the application of the event filter.

TABLE I STATISTICS OF β BEFORE AND AFTER THE EVENT FILTER

Event Filter	Correlation coefficient	β	β_{max}	β_{min}	Std
Before	0.467	1991	5164	1097	952.51
After	0.822	2541	2938	1933	360.97

The improvement in correlation coefficient, the narrowed range between β_{max} and β_{min}, and the reduced standard deviation indicate the effectiveness of the event filter successfully mitigating the impact of these factors on the observed primary frequency response. Applying such filters to all evaluation periods will yield a more consistent and fair comparison of primary frequency response across the years. Such a technique will be used in our future studies to complete an effective decade-long evaluation of the trends in primary frequency response in the Eastern Interconnection.

B. *Improved MW estimation*

Now that the pre-disturbance frequency is recognized as one of the most significant factors that impact the exhibition of the primary frequency response, it should be considered in the MW estimation process when a disturbance hits the disturbance alert system. In this study, we take the event data in 2018 – 2019 for calibration of the parameters, and the events in 2020-2021 for validation of the improved MW estimation method.

Similar to (1), the relationship between the expected $\hat{\beta}$ and pre-disturbance frequency f_{pre} can be obtained through curve fitting with generation trip events that happened in 2018 and 2019:

$$\hat{\beta} = -564.9 f_{pre} + 2186 \quad (4)$$

where the pre-disturbance frequency f_{pre} is normalized with its mean of 60, and standard deviations of 0.01315.

In this study, generation trip events in year 2020 and 2021 are used for validation of the MW estimation performance. The estimated MW size is calculated with the $\hat{\beta}$ corrected with f_{pre}:

$$\widehat{MW} = \hat{\beta}(f_{pre}) \cdot \Delta f \quad (5)$$

Statistics of the MW estimations of events in 2020 and 2021 are shown in Table II.

TABLE II ERROR OF MW ESTIMATION WITH AND WITHOUT f_{pre} CORRECTION

$\hat{\beta}$ correction	Average $\lvert MW\ error \rvert$	$\lvert MW\ error \rvert$ Std
Before	264.0	167.7
After	189.5	130.6
Improvement	28.2%	22.1 %

Both the average and the spread of the MW estimation improved significantly with the simple correction added to the expected primary frequency response $\hat{\beta}$. It is noted that most of the disturbances have pre-disturbance frequencies close to 60 Hz. However, the benefit of the f_{pre}-based correction to $\hat{\beta}$ is most evident in events starting from unusually high or low frequencies.

For example, the event shown in Fig. 7 is a generation trip that happened in Ohio, USA on February 5, 2020 with a size of 857 MW. The event started with a pre-disturbance frequency of 59.986 Hz, which is 14 mHz below the nominal operating frequency. Table III compares the estimated $\hat{\beta}$ and $\widehat{MW}$, as well as the error before and after the application of β correction with f_{pre}.

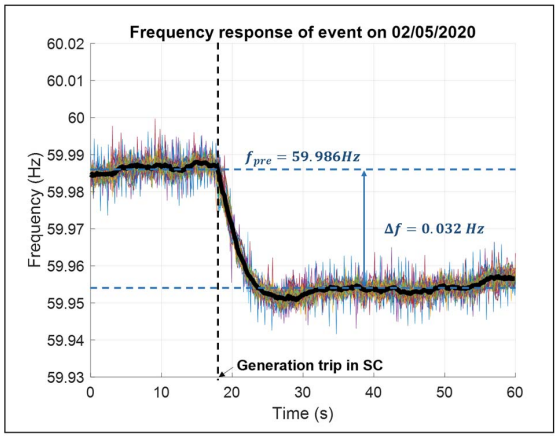

Figure 7 Example event with a low pre-disturbance frequency

TABLE III COMPARISON OF MW ESTIMATES BEFORE AND AFTER $\hat{\beta}$ CORRECTION

$\hat{\beta}$ Correction	$\hat{\beta}$ (MW/0.1Hz)	$\widehat{MW}$	Error
Before	2186	699	-158 MW
After	2787	892	35 MW

Accounting for the impact of the low pre-disturbance frequency on the exhibition of the primary frequency response of the system, the primary frequency response estimate was leveled up by about 601 MW/0.1 Hz, from 2186 MW/0.1Hz to 2787 MW/0.1Hz. The MW size estimate has improved significantly with an absolute error of 35 MW, compared to 158 MW before the correction was made to β.

V. Conclusions

Pre-disturbance frequency and MW size are identified in this paper as two major factors that impact the evaluation of the primary frequency response using generation trip event data. The strong correlation between the exhibited strength of primary frequency response (β) and pre-disturbance frequency and MW size has been presented and the correlation was characterized quantitatively through curve-fitting techniques. Example applications of such knowledge are introduced. This includes screening disturbance events used in primary frequency trending studies for a fair and consistent comparison across the years, as well as improving the event MW size estimation by taking into account the impact of pre-disturbance frequency on the exhibited primary frequency response. Both applications are validated with field measurements in the Eastern Interconnection, collected by the FNET/GridEye system that oversees all major interconnections in North America.

In future works, the event filter based on the pre-disturbance frequency and MW size will be applied in a decade-long trending analysis of the primary frequency response in the Eastern Interconnection. In addition, the MW estimation can be further improved by incorporating season-specific β corrections and iterative MW estimate optimization techniques.

References

[1] *Frequency response standard background document*, NERC Bal-003-1, Nov. 2012.

[2] "Electricity data browser," U.S. Energy Information Administration, [Online]. Available https://www.eia.gov/electricity/data/browser/ (accessed July 26, 2022).

[3] "Fuel mix in ERCOT," Electric Reliability Council of Texas, [Online]. Available https://www.ercot.com/gridinfo/generation (accessed Aug. 31, 2022).

[4] "Power statistics in ENTSO-e," European Network of Transmission System Operators for Electricity (ENTSO-e), [Online]. Available https://www.entsoe.eu/data/power-stats/ (accessed Aug. 31, 2022).

[5] "Variable renewable generation can provide balancing control to the electric power system (fact sheet)," Office of Scientific and Technical Information (OSTI), Department of Energy, [Online]. Available: https://dx.doi.org/10.2172/1094877 (accessed Aug. 31, 2022).

[6] L. Zhu, S. You, H. Yin, Y. Zhao, F. Li, W. Yao, C. O. Reilley, W. Yu, C. Zeng, X. Deng, Y. Zhao, Y. Cui, Y. Zhang, and Y. Liu, "FNET/GridEye: a tool for situational awareness of large power interconnetion grids," in *Proc. IEEE PES Innovative Smart Grid Tech. Eur. (ISGT-Europe),* The Hague, Netherlands, 2020, pp. 379-383.

[7] Y. Zhang, P. Markham, T. Xia, L. Chen, Y. Ye, Z. Wu, Z. Yuan, L. Wang, J. Bank, J. Burgett, R. W. Conners, and Y. Liu, "Wide-area frequency monitoring network (FNET) architecture and applications," *IEEE Trans. Smart Grid*, vol. 1, no. 2, pp. 159-167, Sept. 2010.

[8] M. G. Lauby, J. J. Bian, S. Ekisheva, and M. Varghese, "Frequency response assessment of Eastern and Western Interconnections," in *Proc. North Am. Power Symp. (NAPS)*, Pullman, WA, USA, 2014, pp. 1-5.

[9] J. W. Ingleson and E. Allen, "Tracking the Eastern Interconnection frequency governing characteristic," in *Proc. IEEE PES General Meeting (PESGM)*, Minneapolis, MN, USA, 2010, pp. 1-6.

[10] L. Zhu, Y. Zhao, Y. Cui, S. You, W. Yu, S. Liu, H. Yin, C. Chen, Y. Wu, W. Qiu, M. Mandich, H. Li, A. Ademola, C. Zhang, C. Zeng, X. Jia, W. Wang, H. Yuan, H. Jiang, J. Tan, and Y. Liu, "Adding power of artificial intelligence to situational awareness of large interconnections dominated by inverter-based resources," *High Volt.*, vol. 6, no. 6, pp. 924-937, Oct. 2021.

[11] T. Xia, Y. Zhang, L. Chen, Z. Yuan, P. N. Markham, Y. Ye, and Y. Liu, "Phase angle-based power system inter-area oscillation detection and modal analysis," *Eur. Trans. Electr. Power*, vol. 21, no. 4, pp. 1629-1639, Nov. 2010.

[12] T. Xia, H. Zhang, R. Gardner, J. Bank, J. Dong, J. Zuo, Y. Liu, L. Beard, P. Hirsch, G. Zhang, and R. Dong, "Wide-area frequency based event location estimation," in *Proc. IEEE PES General Meeting (PESGM)*, Tampa, FL, USA, 2007, pp. 1-7.

[13] K. Sun, W. Qiu, Y. Dong, C. Zhang, H. Yin, W. Yao, and Y. Liu, "WAMS-based HVDC damping control for cyber attack defense," *IEEE Trans. Power Syst.*, early access [Online], Apr. 2022. Available: https://ieeexplore.ieee.org/document/9759990

[14] L. Zhu, W. Yu, Z. Jiang, C. Zhang, Y. Zhao, J. Dong, W. Wang, Y. Liu, E. Farantatos, D. Ramasubramanian, A. Arana, and R. Quint, "A comprehensive method to mitigate forced oscillations in large interconnected power grids," *IEEE Access*, vol. 9, pp. 22503-22515, Feb. 2021.

[15] Y. Cui, W. Wang, Y. Liu, P. Fuhr, and M. Morales-Rodriguez, "Spatio-temporal synchrophasor data characterization for mitigating false data injection in smart grids," in *Proc. IEEE PES General Meeting (PESGM),* Atlanta, GA, USA, 2019, pp. 1-5.

[16] Y. Zhao, Y. Dong, L. Zhu, K. Sun, K. Alshuaibi, C. Zhang, Y. Liu, B. Graham, E. Farantatos, B. Marshall, M. Rahman, O. Adeuyi, S. Marshall, and I. L. Cowan, "Coordinated control of natural and sub-synchronous oscillations via HVDC links in Great Britain power system," in *Proc. IEEE PES Transm. Distrib. Conf. Expo. (T&D)*, New Orleans, LA, USA, 2022, pp. 1-5.

[17] H. Xiao, S. Fabus, Y. Su, S. You, Y. Zhao, H. Li, C. Zhang, Y. Liu, H. Yuan, Y. Zhang, and J. Tan, "Data-driven security assessment of power grids based on machine learning approach: preprint," National Renewable Energy Lab. (NREL), Golden, CO, United States, 2020.

[18] Y. Zhao, S. You, M. Mandich, L. Zhu, C. Zhang, H. Li, Y. Su, C. Zeng, Y. Zhao, Y. Liu, H. Jiang, H. Yuan, Y. Zhang, and J. Tan, "Deep learning-based adaptive remedial action scheme with security margin for renewable-dominated power grids," *Energies*, vol. 14, no. 20, p. 6563, July 2021.

[19] C. Zhang, Y. Zhao, L. Zhu, Y. Liu, E. Farantatos, M. Patel, H. Hooshyar, C. Pisani, R. Zaottini, and G. Giannuzzi, "Implementation and hardware-in-the-loop testing of a wide-area damping controller based on measurement-driven models," in *Proc. IEEE PES General Meeting (PESGM)*, Washington, DC, USA, 2021, pp. 1-5.

[20] S. You, J. Zhao, W. Yao, Y. Liu, Y. Cui, L. Wu, J. Guo, and Y. Liu, "FNET/GridEye for future high renewable power grids — applications overview," in *Proc. IEEE PES Transm. Distrib. Conf. Exhib. – Lat. Am. (T&D-LA)*, Lima, Peru, 2018, pp. 1-5.

[21] P. M. Ashton, C. S. Saunders, G. A. Taylor, A. M. Carter, and M. E. Bradley, "Inertia estimation of the GB power system using synchrophasor measurements," *IEEE Trans. Power Syst.*, vol. 30, no. 2, pp. 701-709, July 2014.

[22] P. M. Ashton, G. A. Taylor, A. M. Carter, M. E. Bradley, and W. Hung, "Application of phasor measurement units to estimate power system inertial frequency response," in *Proc. IEEE PES General Meeting (PESGM),* Vancouver, BC, Canada, 2013, pp. 1-5.